Supplementary information for

Multi-layered Polymer Cantilever Integrated with Full-bridge Sensor to Enhance Force Sensitivity in Cardiac Contractility Measurement

Dong-Su Kim[a], Yun-Jin Jeong[a], Jongsung Park[b], Arunkumar Shanmugasundaram[a], and Dong-Weon Lee[a,c,d*]

[a]School of Mechanical Engineering,
Chonnam National University,
Gwangju, 61186, Republic of Korea.

[b]Department of Precision Mechanical Engineering,
Kyungpook National University
Sangju, Gyeongsangbuk-do, 37224, Republic of Korea.

[c]Center for Next-Generation Sensor Research and Development,
Chonnam National University,
Gwangju 61186, Republic of Korea.

[d]Advanced Medical Device Research Center for Cardiovascular Disease.
Chonnam National University,
Gwangju 61186, Republic of Korea.

Corresponding author
Prof. Dong-Weon Lee. Email: mems@jnu.ac.kr

*To whom all correspondence should be addressed.

Table. S1. Various parameters that has been used to achieve maximum cantilever displacement.

S. No	Bottom PI [μm]	Top PI [μm]	Displacement [μm]	Spring Constant [mN/m]
1	12.5	5	305.2	24.1
2	12.5	12.5	125.2	45.2
3	12.5	20	66.7	115
4	12.5	25	46.6	203
5	12.5	30	34	335
6	5	25	92.1	182
7	12.5	25	46.6	203
8	20	25	28.6	273
9	25	25	21.6	362
10	30	25	16.8	493

Table S1 summarize the various parameters that has been used to optimize the cantilever dimension to achieve maximum displacement. Spring constant of the cantilever was calculated using following equation.

$$k = \frac{EWt^3}{4L^3}$$

Where E, W, L, and t are the Young's modulation, width, length and thickness respectively. We investigated the displacement of a cantilever with varying thickness while keeping the length (6000 μm) and width (2000 μm) constant. Firstly, we fixed the bottom PI layer thickness at 12.5 μm while varyied the top PI layer thickness from 5-30 μm. The applied edge load to the cantilever was changed from 0 μm to 100 μm. The cantilever with 5 μm top PI layer thickness exhibited the maximum displacement. However, the neutral plane is not close to the bottom PI layer that we achieved at 25 µm thick top PI layer. The neutral plane close to the bottom PI is desired to produce maximum strain in the top PI layer. As a result, we chose 25 µm as the optimal thickness for top PI layer. Secondly, the cantilevers' displacement was calculated by fixing the top PI layer thickness at 25 µm while varying the bottom PI layer thickness from 5-30 µm. The cantilever produces maximum displacement at 5 µm bottom PI layer thickness. However, we chose 12.5 µm as optimized bottom PI layer thickness as we attained suitable natural plane at that thickness. Based on the FEM based analysis we chose the 12.5 µm bottom PI layer thickness and 25 µm top PI layer thickness are the optimized thickness to produce maximum cantilever displacement that produce higher output voltage.

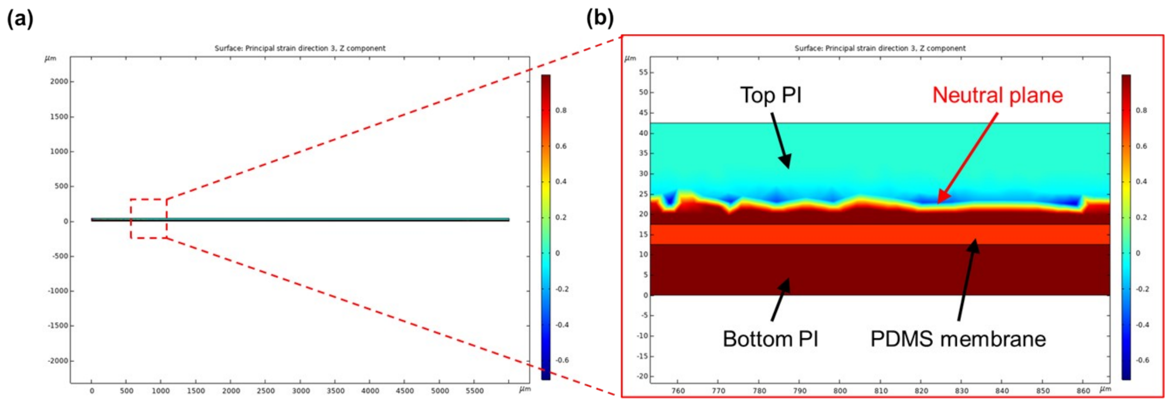

Fig. S1. (a, b) Finite element analysis of the strain along the multilayered cantilever cross-section.

Besides, we have investigated the effect of sandwiched PDMS and encapsulation PDMS layer on the neutral plane of the PI cantilever using FEM based simulation analysis. Fig. S1 in the supplementary shows FEM based analysis of the strain along the cantilever cross-section. Controlling the neutral plane is crucial in designing a reliable multilayered polymer cantilever, where the bending strain imposed on the individual layers that are positioned closer to the neutral plane can be significantly increased. The multilayered cantilever structure consists of bottom PI layer, sandwiched PDMS layer, top PI and encapsulation PDMS layer. Therefore, the neutral plane of the multilayered cantilever is determined by the thickness of each layer and Young's modulus of each materials. When increasing the top PI layer thickness, neutral plane position shifts towards the bottom PI layer resulting in an increase of bending strain in the top PI layer with a typical multilayer structure. The increasing bending strain on the top PI layer is desired to enhance or maximize the strain sensor output voltage. However, 25 µm thick top PI and 12.5 μm bottom PI layer resulting in a optimum natural plane and cantilever displacement. The encapsulation PDMS layer and the sandwiched PDMS layer does not affect significantly to the neutral plane of the multilayered cantilever owing to the low Young's modulus (0.6 MPa) compared to the PI (5 GPa) (Fig. S2).

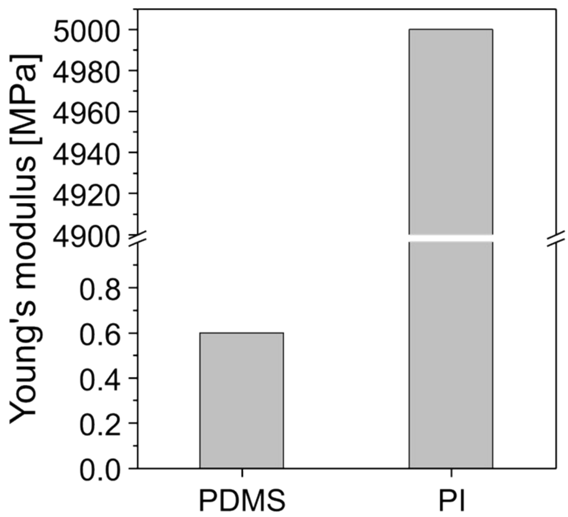

Fig. S2. Bar plot shows the comparison of the Young's modulus of PDMS and PI materials.

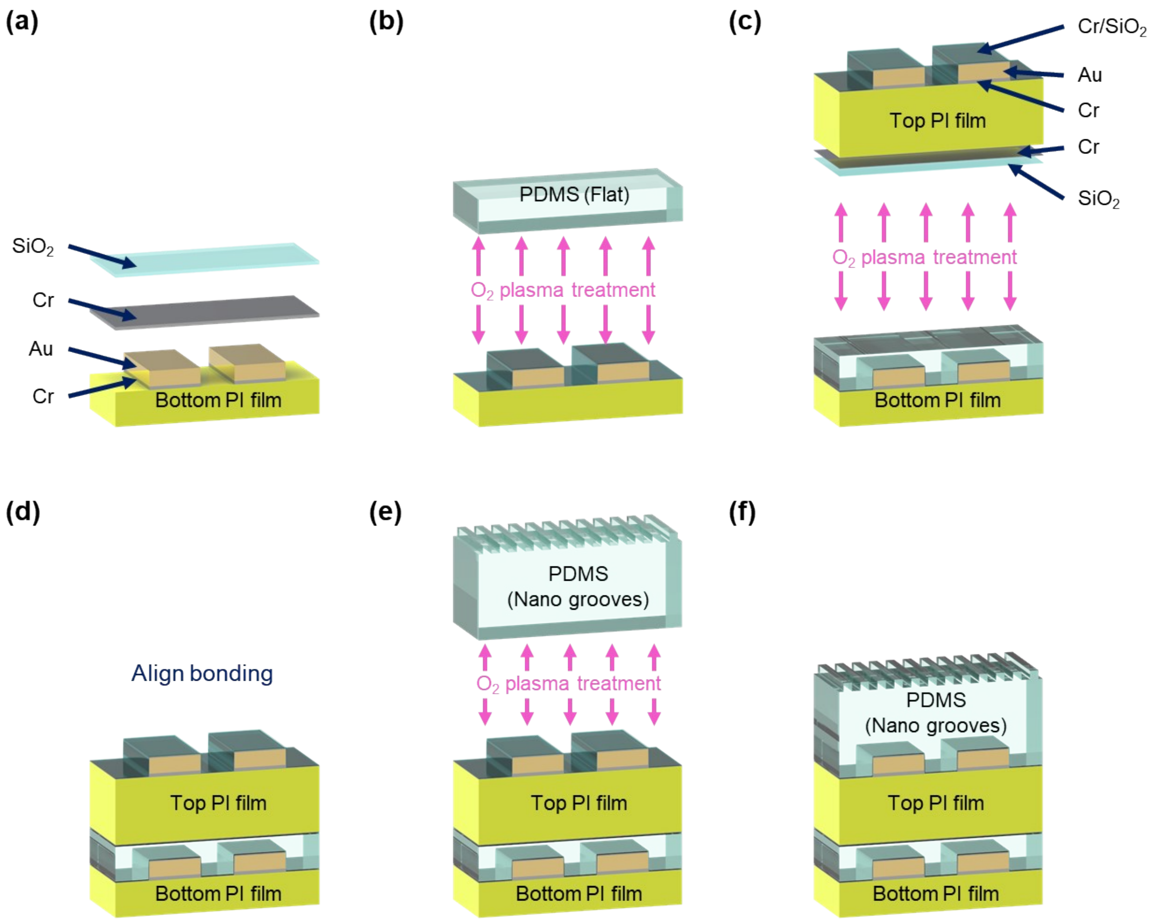

Fig. S3. Cross-sectional view of the multi-layered polymer cantilever fabrication process.

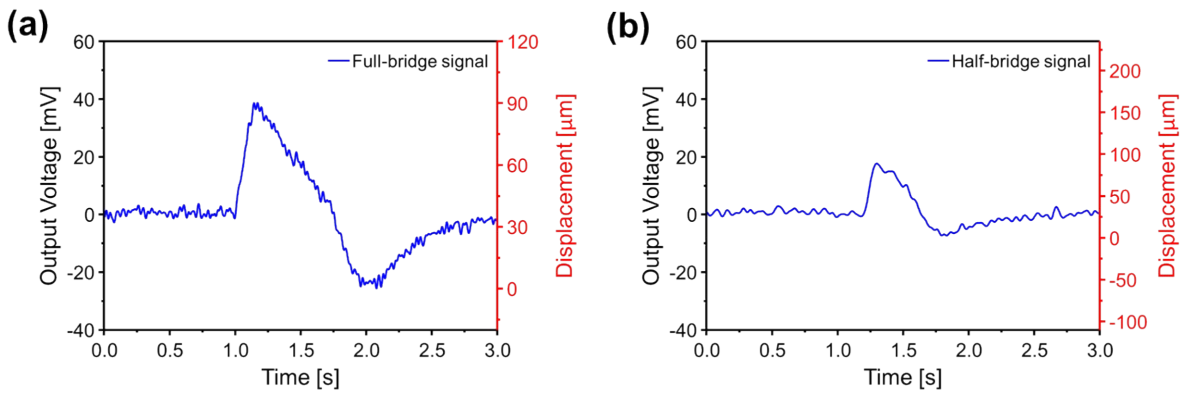

Fig. S4. Representative traces of real-time change in output voltage and displacement of the multi-layered polymer cantilever owing to the contraction and relaxation of different (a) Full-bridge and (b) Half-bridge configurations

Table. S2. Sensing performance of the proposed strain sensor integrated multi-layered cantilever and that of other published strain sensor integrated cantilever based biosensing platforms.

Device types	Measurement method	Sensitivity	Ref.
Piezoresistive sensor integrated PDMS cantilever	Piezoresistive sensor (Ti/Au)	16.3 $\mu\Omega$ μm^{-1}	1
Silicone rubber cantilever	Crack based strain sensor (Pt)	Linear interval: 0.52 Ω μm^{-1} Non-linear interval: 3.33 Ω μm^{-1}	2
PI/PDMS hybrid cantilever	Half-bridge configuration strain sensor (Cr/Au)	0.74 mV μm^{-1}	3
Multi-layered polymer cantilever	Full-bridge configuration strain sensor (Cr/Au	2.22 mV μm^{-1}	This work

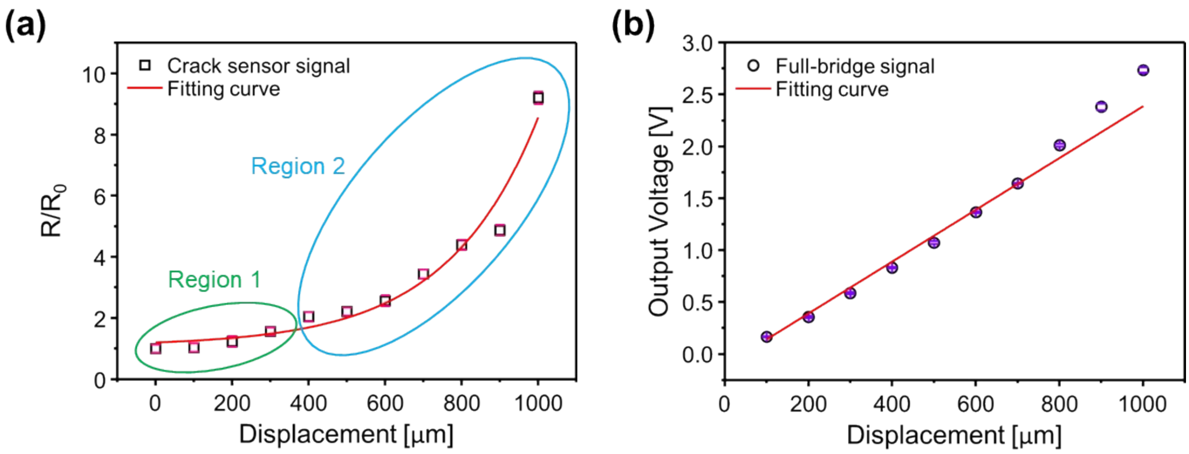

Fig. S5. (a) Change in resistance ratio of the crack sensor integrated silicone rubber cantilever during loading and unloading of applied strain in the tensile range of 0-0.5%. (b) Full-bridge configuration integrated multi-layered polymer cantilever output voltage with respect to applied displacement.

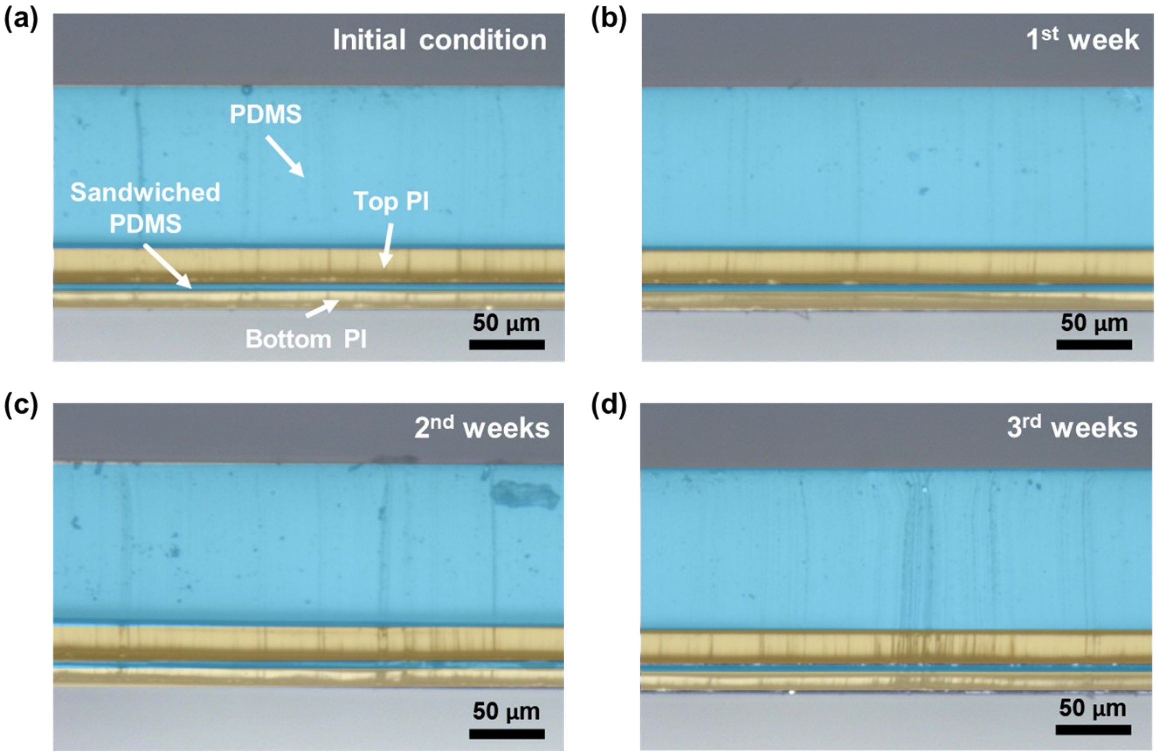

Fig. S6. (a-d) Optical images of the fabricated multi-layered PI/PDMS cantilever before and after immersion in a culture media for 3 weeks.

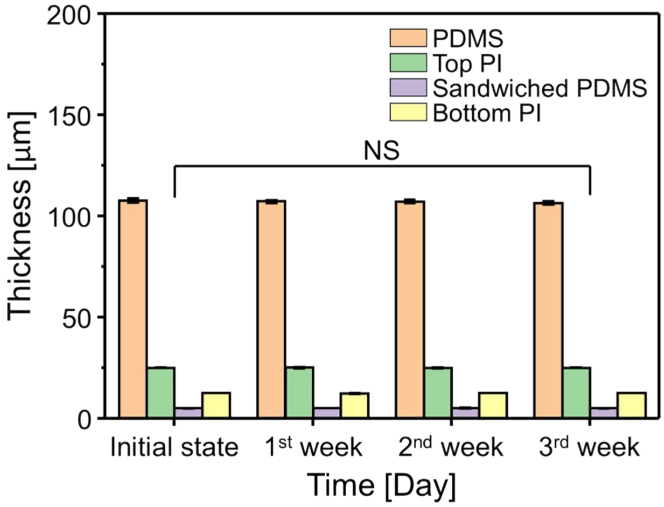

Fig. S7. Bar plot shows the average film thickness of each layer such as bottom PI, top PI, sandwiched PDMS and encapsulation PDMS layer before and after immersion in a culture media for 3 weeks. NS. Non-significant.

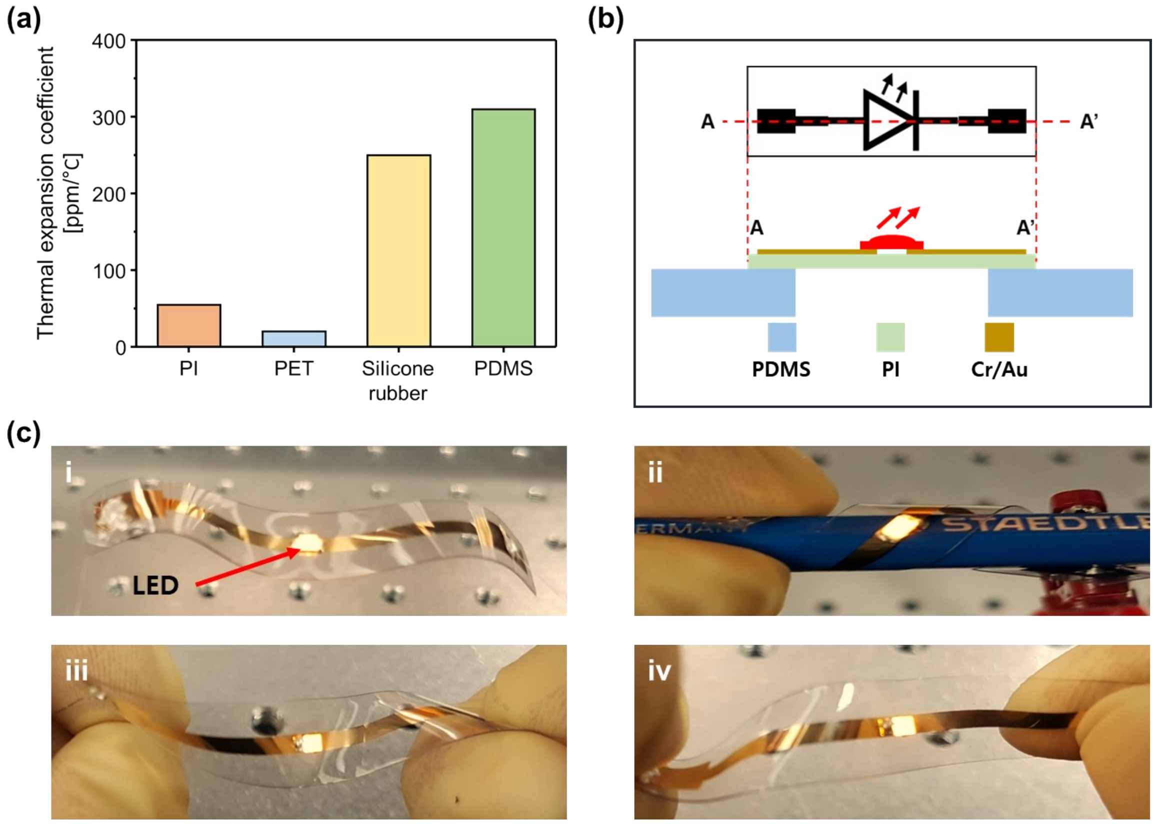

Fig. S8. (a) Bar plot shows the thermal expansion coefficient of different materials such as PI, PET, silicone rubber and PDMS. (b) Schematic illustration of flexible electrode. (c) Photograph demonstrating the flexibility of the fabricated Cr/Au electrode patterned PI substrate.

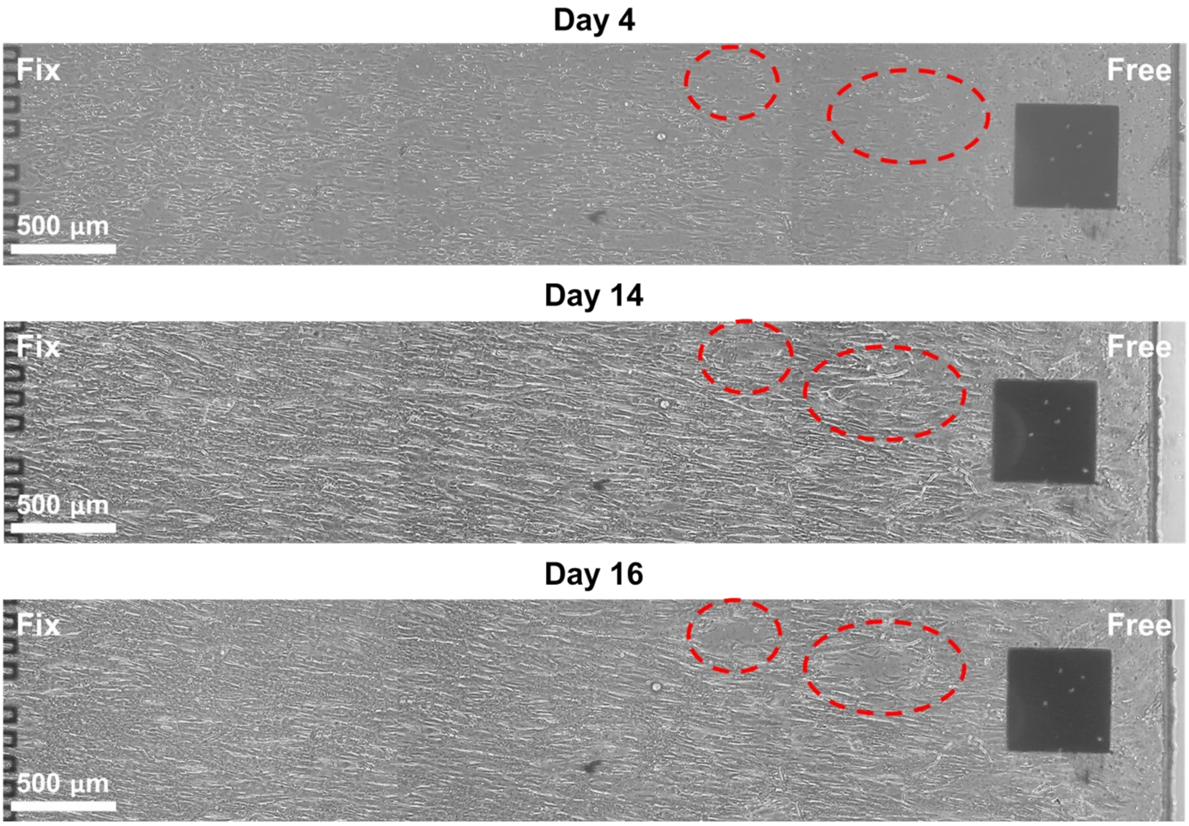

Fig. S9. Morphology of the cardiomyocytes. Optical images of the multi-layered polymer cantilever integrated with the full-bridge configuration and cardiac cells grown at different parts of the nano groove patterned PDMS substrate (Fixed, middle, and free ends of the cantilever).

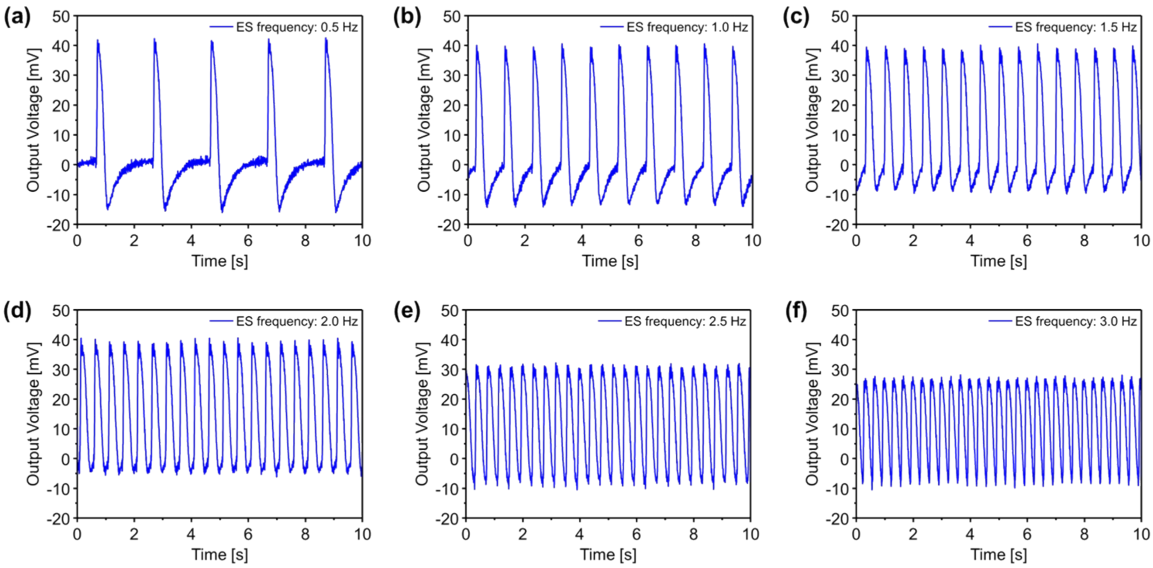

Fig. S10. Effect of external electrical stimulation (ES) on the cultured cardiomyocytes. (a-f) Force-beating frequency relationship in cultured cardiomyocytes under different conditions of electrical stimulation ranging from 0.5 to 3.0 Hz.

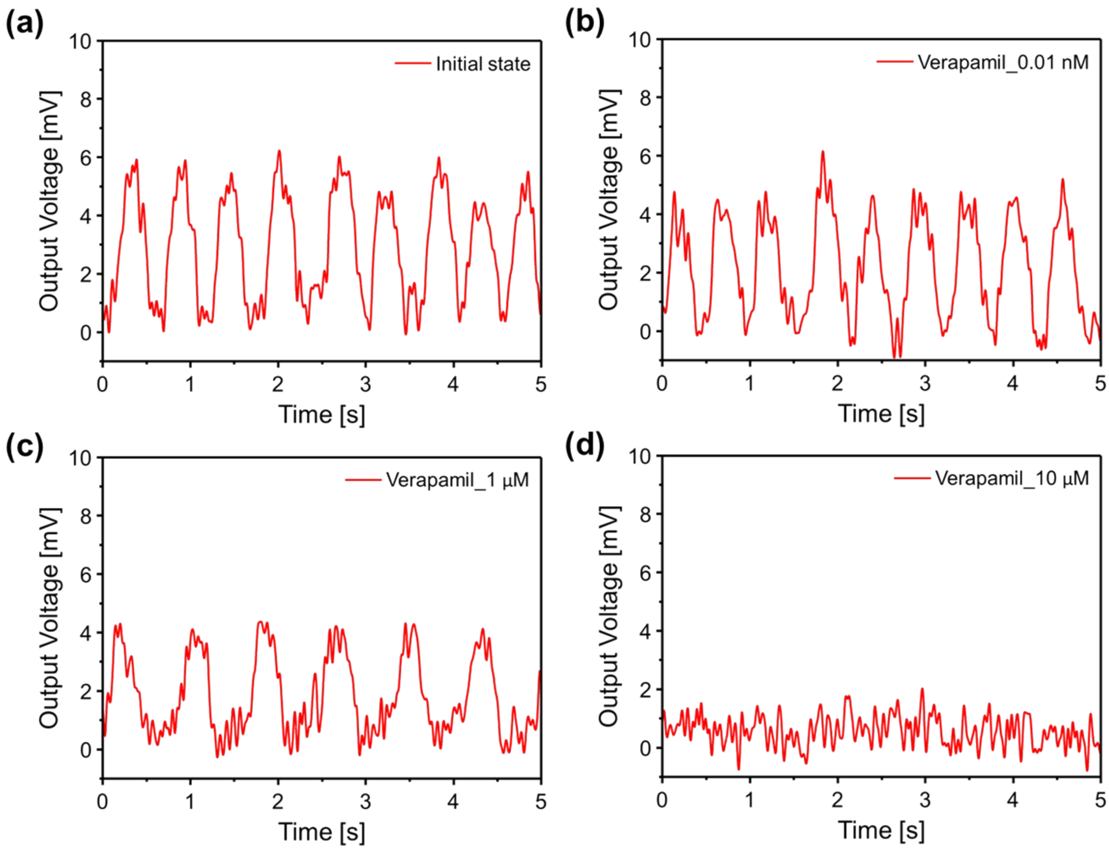

Fig. S11. (a-d) Representative real-time traces of change in sensor output voltage owing to the contraction and relaxation of the different concentrations of Verapamil treated cultured hiPSC-CMs.

References

1. D.-S. Kim, Y.-J. Jeong, B.-K. Lee, A. Shanmugasundaram and D.-W. Lee, *Sensors and Actuators B: Chemical*, 2017, **240**, 566-572.
2. D.-S. Kim, Y. W. Choi, A. Shanmugasundaram, Y.-J. Jeong, J. Park, N.-E. Oyunbaatar, E.-S. Kim, M. Choi and D.-W. Lee, *Nature communications*, 2020, **11**, 1-13.
3. D.-S. Kim, Y.-J. Jeong, A. Shanmugasundaram, N.-E. Oyunbaatar, J. Park, E.-S. Kim, B.-K. Lee and D.-W. Lee, *Biosensors and Bioelectronics*, 2021, 113380.